Available online at www.sciencedirect.com
SCIENCE DIRECT®
Polymer 45 (2004) 3511–3518
polymer
www.elsevier.com/locate/polymer

Crystallization kinetics and morphology of nylon 1212

Minqiao Ren[a], Zhishen Mo[a,*], Qingyong Chen[a], Jianbin Song[a], Shuyun Wang[a], Hongfang Zhang[a], Qingxiang Zhao[b]

[a]*State Key Laboratory of Polymer Physics and Chemistry, Changchun Institute of Applied Chemistry, Chinese Academy of Sciences, Changchun 130022, People's Republic of China*
[b]*College of Materials Engineering, Zhengzhou University, Zhengzhou 450052, People's Republic of China*

Received 12 August 2003; received in revised form 2 March 2004; accepted 9 March 2004

Abstract

The isothermal and non-isothermal crystallization processes of nylon 1212 were investigated by polarized optical microscopy. The crystal growth rates of nylon 1212 measured in isothermal conditions at temperatures ranged from 182 to 132 °C are well comparable with those measured by non-isothermal procedures (cooling rates ranged from 0.5 to 11 °C/min). The kinetic data were examined with the Hoffman–Lauritzen nucleation theory on the basis of the obtained values of the thermodynamic parameters of nylon 1212. The classical regime I → II and regime II → III transitions occur at the temperatures of 179 and 159 °C, respectively. The crystal growth parameters were calculated with (100) plane assumed to be the growth plane. The regime I → II → III transition is accompanied by a morphological transition from elliptical-shaped structure to banded spherulite and then non-banded spherulite. The development of morphology during isothermal and non-isothermal processes shows a good agreement.

Keywords: Nylon 1212; Crystal growth rate; Morphology

1. Introduction

Nylon 1212 is an important industrial polyamide with rather long alkane segments between amide groups. Jones et al. [1–2] observed the morphology and structure of solution-grown, chain-folded lamellar crystals of nylon 1212. Two forms were identified in room temperature and their unit cell dimensions were reported: the triclinic α-form ($a = 0.490$ nm, $b = 0.521$ nm, $c = 3.23$ nm, $\alpha = 50°$, $\beta = 77°$, $\gamma = 64°$) and the triclinic γ-form ($a = 0.490$ nm, $b = 0.802$ nm, $c = 3.23$ nm, $\alpha = 90°$, $\beta = 77°$, $\gamma = 67°$). Li et al. [3] observed the α-form transforms into the γ-form at about 130 °C when the melt-crystallized nylon 1212 sample is heated from room temperature to a higher temperature. This transformation temperature is much lower than that of solution-crystallized nylon 1212 samples [1]. In addition, nylon 1212 was found to isothermally melt-crystallize into the γ-form at higher temperature. Upon further cooling from the crystallization temperature to room temperature, the reverse transformation from the γ-form to α-form occurs.

The crystallization process affects polymer properties through the morphology formed and the extent of crystallization during the solidification process. An important aspect of the crystallization process is its kinetics, both from the fundamental view of polymer physics and for the modeling and control of polymer processing operations. Most frequently, the investigations are conducted under isothermal conditions because of the convenience of the theoretical treatment of the data. However, practical processes such as extrusion, injection molding, and film production usually proceed under dynamic non-isothermal crystallization conditions. In order to reach the optimum condition in an industrial process and to obtain products with better properties, it is necessary to estimate the kinetic parameters of the non-isothermal process. Moreover, from a scientific point of view, the study of crystallization in non-isothermal conditions may expand our general understanding of the crystallization behavior of polymers. Liu et al. [4] studied the isothermal and non-isothermal crystallization kinetics of nylon 1212 by using differential scanning calorimetry (DSC). It was suggested that the development of spherulites, both in terms of nucleation and growth, is described accurately by polarized optical microscopy

* Corresponding author. Tel.: +86-4315262159; fax: +86-4315262126.
E-mail address: mozs@ciac.jl.cn (Z. Mo).

0032-3861/$ - see front matter © 2004 Elsevier Ltd. All rights reserved.
doi:10.1016/j.polymer.2004.03.027

(POM), while DSC data more precisely reflect the overall rate of crystallization. The spherulites in many nylons were investigated [5] and the kinetics of spherulitic crystallization of some nylons was analyzed [6–7]. However, little attention has been paid on the crystallite morphology and crystallization kinetics of nylon 1212.

In this present study, the crystallization processes and morphology of nylon 1212 were investigated by POM equipped with a hot stage device and a computer controlled CCD-camera. Measurements of the crystal growth rates of nylon 1212 were preformed under a wide range of experimental conditions during isothermal and non-isothermal processes. The kinetic data were examined with the Hoffman–Lauritzen nucleation theory [8] on the basis of the obtained values of the equilibrium thermodynamic parameters of nylon 1212.

2. Experimental

2.1. Material

Nylon 1212 granules were provided by Zibo Guangtong Chemical Co. Ltd (China) with the intrinsic viscosity of 1.76 dl/g determined by viscosimetry in H_2SO_4 (96%) at 25 °C. The DSC trace shows the glass transition temperature, $T_g = 46$ °C, and the melting point, $T_m = 186$ °C, respectively. All the samples were carefully dried in a vacuum oven at 70 °C for 24 h before investigation.

2.2. Sample preparation

The isothermally melt-crystallized nylon 1212 samples were prepared by melt-compressed at 220 °C for 5 min, then isothermally crystallized at the designated temperatures for 5 h.

2.3. Wide-angle X-ray diffraction (WAXD)

WAXD experiments were performed at room temperature using a Rigaku D/max 2500V PC X-ray diffractometer. The system consists of an 18 kW rotating-anode generator with a cooper target and a wide-angle power goniometer fitted with a high-temperature attachment. The generator was operated at 40 kV and 200 mA. WAXD data were collected from $2\theta = 5 \sim 35°$ in a fixed time mode with a step interval of 0.02°. During the heating process, the sample was heated at the rate of 4 °C/min to the desired temperature and held there for 2 min before commencing the data collection.

2.4. Density measurements

The density of sample was measured by a suspension method in an alcohol/carbon tetrachloride mixed solution with a PZ-B-5 liquid-density balance.

2.5. Differential scanning calorimeter (DSC)

A differential scanning calorimeter (Perkin–Elmer DSC-7) was used to follow the melting process of nylon 1212 samples at heating rate of 10 °C/min. All DSC runs were performed under a nitrogen purge. Samples with weights in the range of 6.5–7 mg were adopted.

2.6. Polarized optical microscopy (POM)

The morphology and crystallization kinetics of nylon 1212 under isothermal and non-isothermal conditions were investigated by a Leica DMLP polarizing microscope equipped with a Linkam TM600 hot stage and a computer controlled CCD-camera. A small amount of nylon 1212 was sandwiched between two microscopic cover glasses and then placed on the hot stage. The samples were heated quickly (at 80 °C/min) to 220 °C. Kept in this state for 5 min to eliminate any thermal and mechanical history, then cooled quickly to the designated temperatures for isothermal crystallization or cooled at constant cooling rates for non-isothermal crystallization. The development of the morphology and the radius of spherulite were recorded as a function of time or temperature during crystallization process and the data were saved for later analysis.

3. Results and discussion

3.1. Equilibrium thermodynamic parameters

The equilibrium melting enthalpy ΔH_m^0 and the equilibrium melting temperature T_m^0 are two important thermodynamic parameters in determining the crystal growth parameters such as the lateral surface free energy, the fold surface free energy, and the work of chain folding, of semicrystalline polymers. As for polyamides, well-established thermodynamic parameters exist for nylon 6 and nylon 66 [9]. However, as to nylon 1212, these parameters have so far not been correctly determined.

3.1.1. Equilibrium melting enthalpy

Fig. 1 shows a series of WAXD patterns for nylon 1212 samples isothermally melt-crystallized at different temperatures. It is evident that the α and γ-forms can coexist in the same crystallite. The weight fractions of two forms are dependent on the crystallization temperature. The γ-form dominates in the samples crystallized at temperature below ca. 110 °C, while the α-form dominates in the samples crystallized at the temperature from 157 to 177 °C. From the kinetic point of view, the change in the weight fractions of two forms may be attributed to the temperature dependence of the crystallization rate of two forms [10]. Thus, it is reasonable to suppose that the crystallization rate of the α-form becomes larger than that of the γ-form with increasing temperature and becomes dominant above ca. 150 °C in the

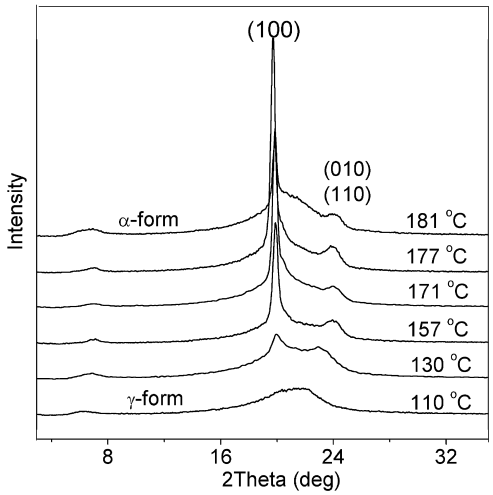

Fig. 1. Series of WAXD patterns for nylon 1212 samples isothermally melt-crystallized at different temperatures for 5 h.

melt crystallization. The crystallization rates of the two forms are about the same in the temperature range from ca. 120 to 140 °C. The rate for γ-form becomes dominant below ca. 110 °C. When the crystallization temperature is above 180 °C, the formation of the α-form is dominant as mentioned above, but the crystallization rate is small. Therefore a large amount of disordered material is present at relatively short isothermal times. This disordered material seems to crystallize in the γ-form and affects the weight fraction of the α-form in the sample. So, in order to obtain the thermodynamic parameters of α-form, we chose the samples crystallized at temperature from 157 to 177 °C.

The DSC melting curves of nylon 1212 samples isothermally melt-crystallized at temperature from 157 to 177 °C are shown in Fig. 2. The multiple DSC curves arise for the samples crystallized at temperature below 169 °C. Peak III is at approximately the same position, regardless of the temperatures at which the samples were crystallized. Peak I is presented in all samples at about 10 °C above

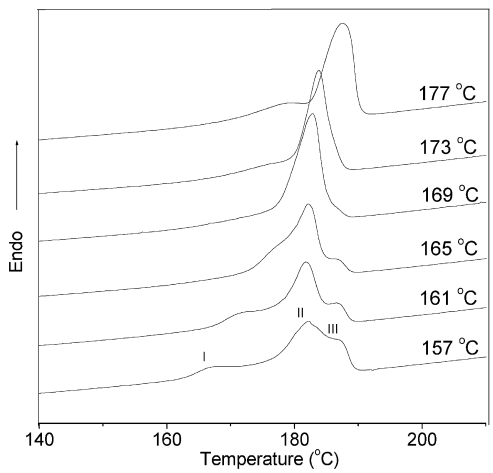

Fig. 2. DSC melting curves of nylon 1212 samples isothermally melt-crystallized at different temperatures for 5 h (heating rate 10 °C/min).

crystallization temperature. It moves more sharply to higher temperature than peak II. Multiple endotherms phenomenon is a very common observation in thermal studies of nylons [4,11–12]. These studies have proven conclusively that the highest melting peak corresponds to melting of the recrystallized material while the other melting endotherms are related to the melting of lamellae with different thickness developing under different crystallization conditions. So the cause of peak I is assumed to be microcrystallite formation in the boundary layer between the larger crystallites, and peak III corresponds to the melting of the ultimate metastable crystals in given condition. The area of peak II is much larger than that of peak I or peak III, which indicates that peak II is caused by the melting of the major crystal. When crystallization temperature is above 169 °C, melting recrystallization does not occur on heating.

Even though the multiple endotherms of nylon 1212 were attributed to the melting of the crystals with different crystal perfection. However, when nylon 1212 displaying different crystal forms are concerned, the multiple endotherms may also be related to the respective melting of the different crystal forms. Fig. 3 shows a series of WAXD patterns in a continuous heating process for the isothermally melt-crystallized nylon 1212 sample. The (100) and (010/110) doublet diffraction peaks gradually approached each other as the temperature increased but never merged into one before melting. This gave the proof that no crystal transition occurred in the melting range of nylon 1212. Therefore, the possibility that the multiple endotherms result from different crystal forms can be ruled out.

An approach of extrapolating the linear relationship between the melting enthalpy ΔH_m and the specific volume V_{sp} of samples with different degrees of crystallinity to the 100% crystalline condition V_{sp}^c was adopted to determine ΔH_m^0 for nylon 1212 [9]. The original melting enthalpy ΔH_m (areas of peak I and peak II) was obtained by resolving overlapping peaks with the Gaussian function. The specific volume V_{sp} was measured with a PZ-B-5 liquid-density

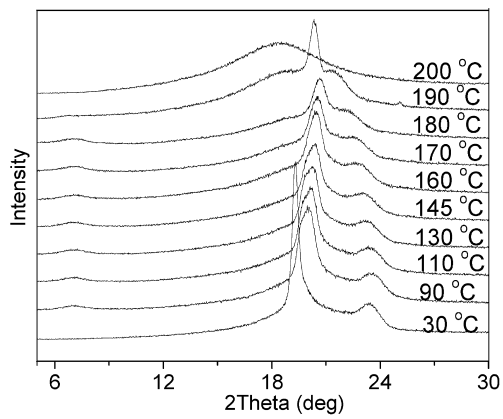

Fig. 3. Series of WAXD patterns in a continuous heating process for the nylon 1212 sample isothermally melt-crystallized at 155 °C for 5 h.

balance. Fig. 4 shows the plot of ΔH_m against V_{sp} for nylon 1212 samples. Through linear regression, a linear plot of melting enthalpy versus specific volume was obtained. The α-form unit cell of nylon 1212 gives a calculated density ρ_c of 1.156 g/cm^3 and the specific volume V_{sp}^c of 0.865 cm^3/g, respectively. If V_{sp}^c of a hypothetical 100% crystalline nylon 1212, i.e. 0.865 cm^3/g was substituted for V_{sp}, the $\Delta H_m^0 = 292.2$ J/g was derived.

For polyamides, a procedure to estimate the ΔH_m^0 based on the additivity of properties [13] was used as an approximation [14]. Xenopoulos et al. [15] normalized the given group contributions and gave values of 3.8 and 5.0 kJ/mol for the amide and methylene group, respectively. Using these contributions, approximate equilibrium melting enthalpy for all polyamides can be calculated. The value of $\Delta H_m^0 = 117.6$ kJ/mol (298 J/g) was obtained for nylon 1212. It is evident that this value is very close to the value of 292.2 J/g obtained by $\Delta H_m - V_{sp}$ method. Based on the additivity of properties, for polyamide, the value of ΔH_m^0 increases with increasing number of methylene groups present in the repeating unit. Therefore the value of ΔH_m^0 obtained by $\Delta H_m - V_{sp}$ method for nylon 1212 (292.2 J/g) should be reasonable compared with nylon 66 (45 cal/g or 188.3 J/g) [16], nylon 610 (50.6 cal/g or 211.7 J/g) [17] and nylon 1010 (58.3 cal/g or 244.0 J/g) [18].

3.1.2. Equilibrium melting temperature

Liu et al. [4] obtained that the value of $T_m^0 = 188.0$ °C for nylon 1212 by using Hoffman–Weeks approach [19]. However, this value seems to be lower for it is very close to the melting temperature of the metastable crystal, 186 °C. As the sensitivity of T_m^0 to the chosen crystallization condition is appreciable, we chose the crystallization temperature ranged from 169 to 177 °C and the crystallization time was 5 h. Representative DSC melting curves of nylon 1212 samples are also shown in Fig. 2. As peak II is the main crystal peak, the value of T_m^0 was determined to be 204.7 °C by extrapolation of the melting temperature T_m (II) versus crystallization temperature T_c (Fig. 5).

For polyamides, the value of T_m^0 is related to the intrachain amide density. The larger the intrachain amide density, the higher the value of T_m^0. Based on this property, the value of T_m^0 decreases with increasing number of methylene groups present in the repeating unit. Therefore the value of $T_m^0 = 204.7$°C for nylon 1212 should be reasonable compared with nylon 66 (280 °C) [9], nylon 610 (238 °C) [20] and nylon 1010 (214 °C) [18].

3.2. Isothermal growth rate

The crystal growth rate G is the rate of macroscopic advance of the crystal front in one direction. With only a few exceptions [21–24], at a fixed temperature, the plot of radius r versus time t is linear and its slope gives the value of G at the selected temperature for the measurement. Representative examples of radius as a function of time at different crystallization temperatures for nylon 1212 are shown in Fig. 6. It is evident that the linear relationships between radius and time are very well. As expected, the growth rate increases with decreasing crystallization temperature.

It is worthy to note that the sample thickness and the previous thermal history can affect the subsequent crystallization. A clear trend to more rapid crystallization in thinner films can be seen. With the melting temperature increases and the time at the melting increases, the growth rate decreases [6]. So, in order to obtain the reliable mechanism of crystallization for this polymer, the samples were in the same thickness and the isothermal and non-isothermal crystallization processes were conducted under the same thermal history. As shown in Fig. 6, the final spherulite diameter of nylon 1212 is above 100 μm, and the sample thickness (about 20 μm) is much less than the spherulite diameter. This indicates that the nylon 1212 samples during isothermal crystallization processes in this study exhibit a two-dimensional growth.

3.3. Non-isothermal growth rate

The isothermal measurements are usually time consum-

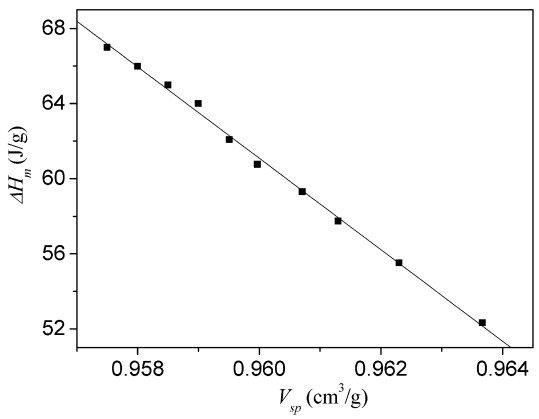

Fig. 4. Determination of equilibrium melting enthalpy ΔH_m^0 for nylon 1212 from the relationship between ΔH_m and V_{sp}.

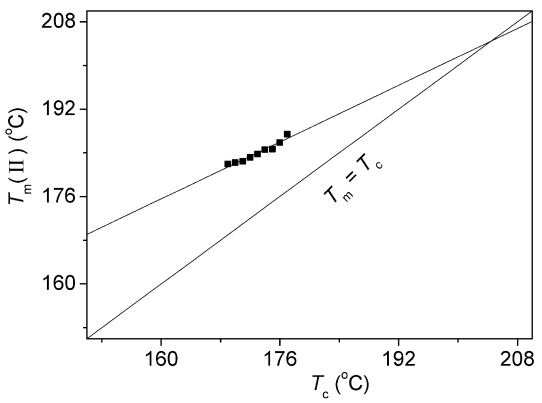

Fig. 5. Application of Hoffman–Weeks approach to nylon 1212 for determining its equilibrium melting temperature T_m^0.

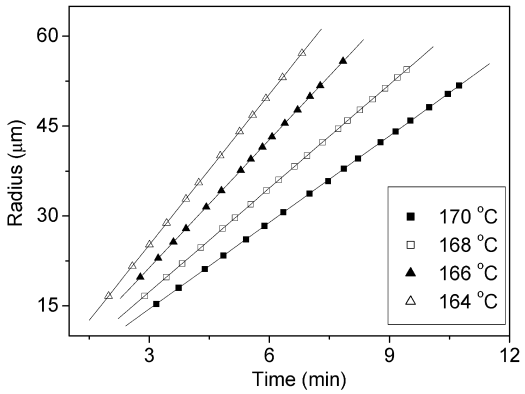

Fig. 6. Radius of spherulite as a function of time at different crystallization temperatures for nylon 1212.

ing, and moreover, polymers usually undergo non-isothermal crystallization processes, especially in practical processing. Therefore, it raises the question of how crystal growth rate measured at constant temperatures can be applied to non-isothermal processes. Chen and Chung [25] first suggested an alternative technique. According to their investigations, by using one single measurement, it is possible to obtain isothermal crystallization data that would require several separate experiments with isothermal methods. This procedure was further developed by Di Lorenzo et al. [26–27] by using various cooling rates and a self-nucleation procedure. In such case, crystallization is monitored during cooling at a constant rate, and crystal growth rate G is estimated by taking the first derivative of the radius of spherulite r versus temperature T plot at each experimental point:

$$G = \frac{dr}{dt} = \frac{dr}{dT}\frac{dT}{dt} \quad (1)$$

Variation of the radius of spherulite with temperature during cooling from the melt at 1 °C/min is shown in Fig. 7. A curve fitting methods was used to fit the radii of the spherulite. Polynomial fitting gave curves that decrease smoothly in the temperature ranges of 163–174 °C, as shown in Fig. 7. To simplify the calculation of growth rates, we chose a third-order equation which can be written in the form:

$$r = f(T) = a_0 + a_1T + a_2T^2 + a_3T^3 \quad (2)$$

where r is the radius of spherulite as function of temperature T and dr/dT can be obtained by differentiating the above equation with respect to T:

$$\frac{dr}{dT} = f'(T) = a_1 + 2a_2T + 3a_3T^2 \quad (3)$$

According to Eqs. (1)–(3), the growth rate-temperature relation was obtained (Fig. 8).

As shown in Fig. 9, crystal growth rates of nylon 1212 obtained with isothermal crystallization and non-isothermal crystallization using different cooling rates are in good agreement and data obtained with different cooling rates are well connected to each other. Higher cooling rates permits to obtain growth rates at lower temperatures. So, with the non-isothermal method, growth rates can be measured at rather lower temperatures. Unfortunately, the use of high cooling rates increases the risks of thermal lags and temperature gradients within the samples. A few studies relating the influence of sample thickness and cooling rate to the occurrence of thermal gradients during non-isothermal condition have been reported in the literature [28–29]. Owing to the thermal lags, transition can occur at temperatures that do not correspond to those detected by the instrumentation, the thicker is the sample, and the higher is the cooling rate, the more critical this problem is [30]. For these reasons, in order to obtain reliable values of crystal growth rates, cooling rates as well as sample thickness should be limited. The samples used in this study were very flat and the thickness is about 20 μm. We chose the cooling rate ranged from 0.5 to 80 °C/min. However, the results showed that the values of crystal growth rates obtained from the cooling rates higher than 11 °C/min are unreasonably high and the values obtained with different cooling rates are not well connected to each other. So, in this study, the cooling rate was chosen below 11 °C/min.

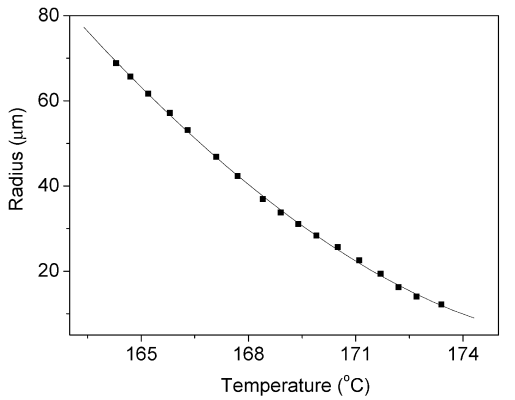

Fig. 7. Variation of the spherulite radius of nylon 1212 with temperature during cooling from the melt at 1 °C/min.

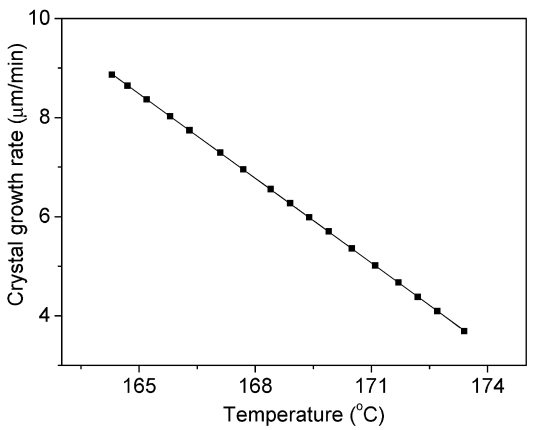

Fig. 8. Variation of the growth rate of nylon 1212 with temperature during cooling from the melt at 1 °C/min.

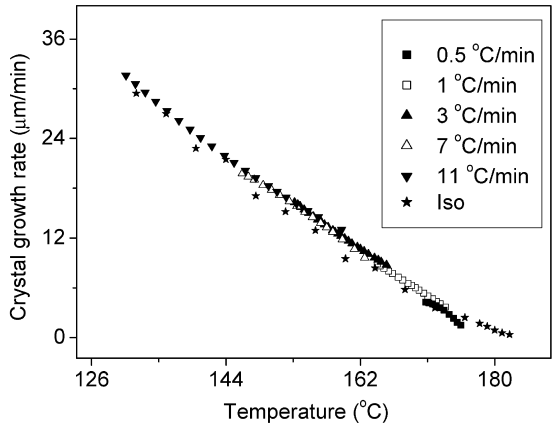

Fig. 9. Crystal growth rates of nylon 1212 during cooling at various rates and under isothermal conditions.

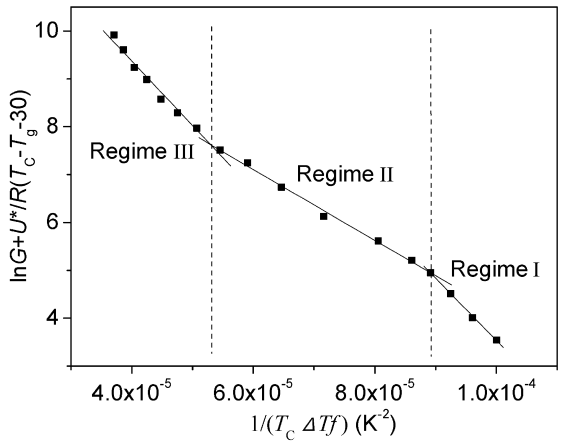

Fig. 10. Analysis of the isothermal growth rate of nylon 1212 as a function of crystallization temperature based on the Lauritzen–Hoffman secondary nucleation theory.

3.4. Regime analysis

According to the Lauritzen–Hoffman secondary nucleation theory [8], the crystal growth rate G of a crystalline aggregate (e.g. spherulite or axialite) for each regimes is dependent on the degree of undercooling ΔT, and is defined by the following equation:

$$G = G_0 \exp\left[-\frac{U^*}{R(T_c - T_\infty)}\right]\exp\left[-\frac{K_g}{T_c \Delta T f}\right] \quad (4)$$

where G_0 is the pre-exponential factor; U^* is the transport activation energy and is usually equal to 1500 cal/mol (6300 J/mol); T_∞ is a hypothetical temperature below which all viscous flow ceases and is usually equal to $T_g - 30$; T_c is the crystallization temperature; ΔT is the degree of supercooling and is equal to $T_m^0 - T_c$, where T_m^0 is the equilibrium melting temperature; f is a correction term to account for the variation in the bulk enthalpy of fusion per unit volume with temperature and is equal to $2T_c/(T_m^0 + T_c)$; K_g is the nucleation parameter and can be defined as follows:

$$K_g = nb_0\sigma\sigma_e T_m^0/\Delta h_f^0 k \quad (5)$$

where $n = 4$ for regimes I and III and $n = 2$ for regime II; b_0 is the thickness of a monomolecular layer in the crystal; σ is the lateral surface free energy; σ_e is the fold surface free energy; k is the Boltzmann constant; and Δh_f^0 is the bulk melting enthalpy per unit volume for a fully crystalline polymer ($\Delta h_f^0 = H_m^0 \rho_c$).

Analysis of the isothermal growth rate of nylon 1212 as a function of crystallization temperature based on the Lauritzen–Hoffman theory is shown in Fig. 10. It clearly exhibits the classical regime I → II and regime II → III transitions at the temperatures of 179 and 159 °C, respectively. The K_{gI}/K_{gII} value is ca. 1.76 and K_{gIII}/K_{gII} value is ca. 1.82, respectively, which is close to theoretical predication of $K_{gI} = K_{gIII} = 2K_{gII}$. The calculated K_g values were listed in Table 1.

3.5. Surface free energy and work of chain folding

The product of $\sigma\sigma_e$, obtained from the derived value of K_g, can be used to calculated σ_e and q. With the procedure of Hoffman et al. [31], σ and σ_e can be determined from the following relationship:

$$\sigma = \alpha(a_0 b_0)^{1/2}\Delta h_f^0 \quad (6)$$

$$\sigma_e = \sigma\sigma_e/\sigma \quad (7)$$

where a_0 is the width of the molecular chain in the crystal; $a_0 b_0$ represents the cross-sectional area of the polymer chain. According to the α-form unit cell of nylon 1212, if the crystal growth plane is on the (100) plane, a_0 should be 0.200 nm and b_0 should be 0.439 nm. α is an empirical constant that is usually between 0.1 and 0.3. In general, α is 0.1 for hydrocarbons such as polyolefins, 0.24 for polyesters, and 0.3 for most organics. For nylon 6 and nylon 66, a reasonable estimate can be made for σ taking $\alpha = 0.1$ [7]. So in this study we took $\alpha = 0.1$ for nylon 1212 in order to make a comparison with the results from other nylons. The values of σ and σ_e for regimes I, II, and III were determined and listed in Table 1.

The work of chain folding q is derived from the fold

Table 1
Kinetic data for isothermally crystallized nylon 1212 calculated from secondary nucleation theory

Parameter	Regime I	Regime II	Regime III
T_g (K)	319.15	319.15	319.15
T_m^0 (K)	477.85	477.85	477.85
Δh_f^0 (J/cm^3)	337.78	337.78	337.78
K_g (K^2)	1.30×10^5	7.4×10^4	1.35×10^5
$\sigma\sigma_e$ (erg^2/cm^4)	722.5	822.5	750.3
σ (erg/cm^2)	10.0	10.0	10.0
σ_e (erg/cm^2)	72.3	82.3	75.0
b_0 (nm)	0.439	0.439	0.439
a_0 (nm)	0.200	0.200	0.200
q (kcal/mol)	1.83	2.08	1.90

surface free energy by

$$q = 2a_0 b_0 \sigma_e \quad (8)$$

The values of q from Eq. (8) for regimes I, II, and III were obtained and listed in Table 1.

q is the work required to bend a polymer chain back upon itself, taking into account the conformational constraints imposed on the fold of the molecular chain. Therefore q is one parameter very closely correlated with the molecular structure, which is one measure of the stiffness of the polymer chain. For polymers of ordinary stiffness, values of q between 1 and 10 kcal/mol of folds are to be anticipated. The q value of ca. 1.83–2.08 kcal/mol obtained in this work for nylon 1212. Magill [7] reported the results for nylon 6 ($\sigma_e = 60$–65 erg/cm^2, $A_0 = 0.177$ nm^2, $q = 3.06$–3.32 kcal/mol) and nylon 66 ($\sigma_e = 40.0$ erg/cm^2, $A_0 = 0.176$ nm^2, $q = 2.03$ kcal/mol). As the structures of these nylons are similar but with different alkane segments between amide groups. The longer alkane segments would make the chain more flexible. Thus one would expect q to decrease because more flexible chain is easier to bend to make the fold. So the average q value of nylon 1212 (1.94 kcal/mol) is relatively reasonable because it is smaller than those of nylon 6 and nylon 66.

3.6. Morphology of crystallite

Fig. 11 shows a series of POM micrographs for nylon 1212 isothermally and non-isothermally melt-crystallized at different temperatures. When nylon 1212 was crystallized at 180 °C, the growing unit takes on an elliptical-shaped or axialite-like structure (Fig. 11(a)) and then it progressively changes into a spherulite-like structure (Fig. 11(b)) with decreasing crystallization temperature. Because the regime I → II transition occurs at 179 °C, the elliptical-shaped structure just occur in the range of regime I. As crystallization temperature is further decreased (regime II), the banded spherulite (Fig. 11(c) and (d)) is formed and the band spacing decreases with decreasing crystallization temperature. At crystallization temperature below 159 °C (Fig. 11(e)) (regime II → III transition temperature), the banded structure disappears. So the regime I → II → III transition was accompanied by a morphological transition from elliptical-shaped structure to banded spherulite and then non-banded spherulite. This phenomenon is in agreement with that reported by Hong et al [32]. The temperature limitation of banded spherulite formation is 159 °C at which the regime II → III transition occurs. This fact may lead us to consider that the foramtion of banded spherulite in nylon 1212 may be related to the regime behavior. In regime II, the crystallization takes place at which the nulceation and substrate completion rates are comparable. This condition is favor to make the lamellae to be well stacked for good spherulite growth. On the other hand, in regime III substrate completion is dominated by nucleation events and many nuclei would lead to disordered crystal growth. Under this condition, the disorganized lamellae are formed with many defects, resulting that good spherulite structure could not be produced. Since it is commonly believed that the periodic extinction of banded spherulite is led by lamellar twist during growth [33], the well-stacked lamellae should be advantageous to form a periodic morphology for banded spherulite. In other words, the distorted lamellar structure formed in regime III and mostly immature and coarse spherulites formed in regime I are difficult to produce periodic twists for forming banded spherulite. Besides, the increase in band spacing with crystallization temperature may be related to larger thickness of lamellae formed at a rather higher crystallization temperature.

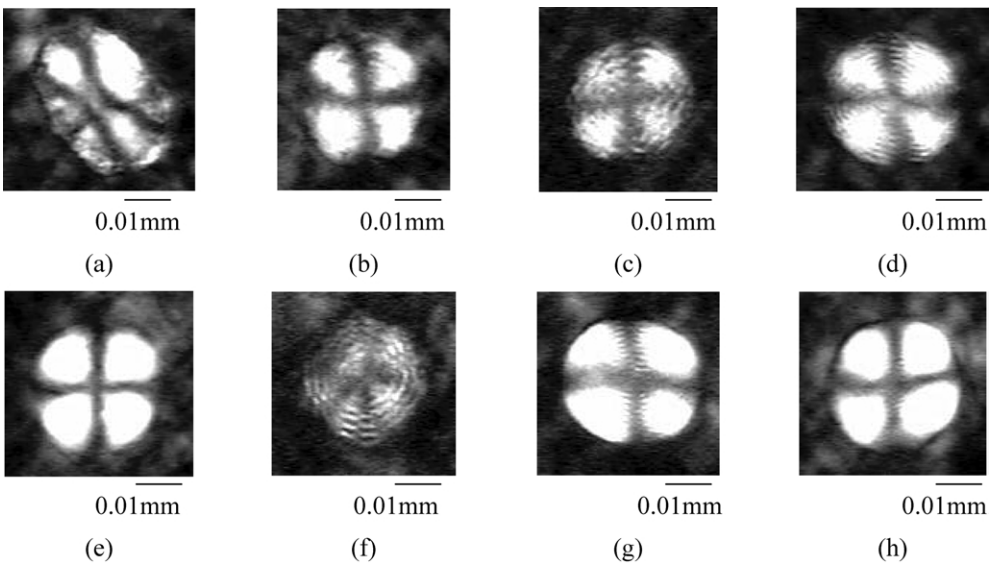

Fig. 11. Representative POM micrographs of nylon 1212 isothermally crystallized at (a) 180 °C; (b) 178 °C; (c) 176 °C; (d) 166 °C; (e) 159 °C and non-isothermally crystallized at cooling rate (f) 1 °C/min; (g) 7 °C/min; (h) 11 °C/min.

In order to observe the development of the morphology during the non-isothermal processes, nylon 1212 samples were cooled from the melt at different rates. Fig. 11(f) shows the morphology of nylon 1212 formed at slow cooling rate (1 °C/min). The center of the irregular spherulite shows an elliptical-shaped structure which was formed at the temperature range from ca. 179 to 181 °C, while the outside part of the spherulite shows the banded structure which was formed at the temperature range from 174 to 178 °C. This indicates a morphological change of nylon 1212 from the elliptical-shaped structure to the banded spherulite with decreasing temperature. With the higher cooling rate (7 or 11 °C/min), the crystallization occurs at the lower temperature range. This may be explained that the mechanism of crystallization is dependent on cooling rate. At slow cooling rates, there is sufficient time to activate nuclei at higher temperatures. On the contrary, at faster cooling rates, the activation of nuclei occurs at lower temperatures. So the elliptical-shaped structure did not appear in Fig. 11(g) and (h). However, it is evident that the banded structure exists at temperature range from ca. 161 to 170 °C (Fig. 11(g)), but disappears completely at temperature range from ca. 155 to 159 °C (Fig. 11(h)). Obviously, the morphological change of nylon 1212 obtained from non-isothermal crystallization and isothermal crystallization shows a good agreement.

Inserting a primary red filter (λ-plate) between the crossed polars, the nylon 1212 crystallites formed at the temperature from 132 to 182 °C exhibit typical positive birefringence (i.e. the first and the third quadrants appear blue while the second and forth quadrants appear yellow). This phenomenon is in accordance with those observed in nylon 6 and nylon 66 [5].

4. Conclusions

Crystallization processes of nylon 1212 under isothermal and non-isothermal conditions were investigated by POM. The crystal growth rates measured under isothermal conditions are well comparable with those measured by non-isothermal procedures (cooling rates ranged from 0.5 to 11 °C/min). The equilibrium melting enthalpy and the equilibrium melting temperature were determined, respectively. The kinetic data were analyzed by the Hoffman–Lauritzen nucleation theory. The classical regime I → II and regime II → III transitions occurred at the temperatures of 179 and 159 °C, respectively. The lateral-surface free energy, the fold-surface free energy, and the work of chain folding were calculated with the (100) plane. The regime I → II → III transition was accompanied by a morphological transition from the elliptical-shaped structure to banded spherulite and then non-banded spherulite. The development of morphology during isothermal and non-isothermal processes shows a good agreement.

Acknowledgements

This work was supported by the National Natural Science Foundation of China (No.270274049 and No. 220374051).

References

[1] Jones NA, Atkins EDT, Hill MJ. J Polym Sci, Part B: Polym Phys 2000;38:1209.
[2] Jones NA, Atkins EDT, Hill MJ. Macromolecules 2000;33:2642.
[3] Li Y, Yan D, Zhou E. Colloid Polym Sci 2002;280:124.
[4] Liu MY, Zhao QX, Wang YD, Zhang CG, Mo ZS, Cao SK. Polymer 2003;44:2537.
[5] Magill JH. J Polym Sci, Part A-2 1966;4:243.
[6] Mclaren JV. Polymer 1963;4:175.
[7] Magill JH. Polymer 1965;6:367.
[8] Lauritzen JI, Hoffman JD. J Appl Phys 1973;44:4340.
[9] Wunderlich B, Macromolecular physics, vol. 3. New York: Academic Press; 1980. Chapter 8.
[10] Kyotani M, Mitsuhashi S. J Polym Sci, Part A-2 1972;10:1497.
[11] Li Y, Zhu X, Tian G, Yan D, Zhou E. Polym Int 2001;50:677.
[12] Franco L, Puiggali J. J Polym Sci, Part B: Polym Phys 1995;33:2065.
[13] Van Krevelen DW. Properties of polymers, 3rd ed. Amsterdam: Elsevier; 1990. Chapter 5.
[14] Xenopoulos A, Wunderlich B. J Polym Sci, Part B: Polym Phys 1990; 28:2271.
[15] Xenopoulos A, Wunderlich B, Subirana JA. Eur Polym J 1993;29: 927.
[16] Starkweather HW, Zoller P, Jones GA. J Polym Sci, Part B: Polym Phys 1984;22:1615.
[17] Jin Y, Chen D. Chin J Appl Chem 1987;4:25.
[18] Mo Z, Meng Q, Feng J, Zhang H, Chen D. Polym Int 1993;32:53.
[19] Hoffman JD, Weeks JJ. J Chem Phys 1962;37:1723.
[20] Wang GM, Yan DY, Bu HS. Chin J Polym Sci 1998;16:243.
[21] Keith HD, Padden FJ. J Appl Phys 1964;35:1286.
[22] Banks W, Hay JN, Sharples A, Thomson G. Polymer 1964;5:163.
[23] Chen M, Chen JY. J Polym Sci, Part B: Polym Phys 1998;36:1335.
[24] Lee CH. Polymer 1998;39:5197.
[25] Chen M, Chung C. J Polym Sci, Part B: Polym Phys 1998;36:2393.
[26] Di Lorenzo ML, Cimmino S, Silvestre C. Macromolecules 2000;33: 3828.
[27] Di Lorenzo ML. Polymer 2001;42:9441.
[28] Monasse B, Haudin JM. Colloid Polym Sci 1986;264:117.
[29] Ding Z, Spruiell JE. J Polym Sci, Part B: Polym Phys 1997;35:1077.
[30] Androsch R, Wunderlich B. Thermochim Acta 2000;364:181.
[31] Hoffman JD, Davis GT, Lauritzen JI. In: Hannay HB, editor. Treatise on solid state chemistry, vol. 3. New York: Plenum Press; 1975. Chapter 6.
[32] Hong PD, Chung WT, Hsu CF. Polymer 2002;43:3335.
[33] Bassett DC. Principles of polymer morphology. Cambridge: Cambridge University Press; 1981. Chapter 2.